ORIGINAL ARTICLE

CrossMark

Full parameters inversion model for mining subsidence prediction using simulated annealing based on single line of sight D-InSAR

Lei Wang[1] · Nan Li[1] · Xian-ni Zhang[1] · Tao Wei[1] · Yuan-fei Chen[2] · Jian-feng Zha[2]

Abstract
Due to the inability of the single line of sight D-InSAR to monitor the three-dimensional deformation of the surface, the conventional methods are unable to obtain the prediction parameters (probability integral parameters) of surface subsidence in coal mining. In this paper, a calculation method of simulated annealing (SA) for probability integral parameters based on single line of sight D-InSAR is proposed. Firstly, the method predicts the subsidence, the horizontal movement in the north–south direction and the horizontal movement in the east–west direction of the target pixel by using the probability integral method. Based on the projection relationship between the three-dimensional deformation and the LOS deformation, the predicted movement and deformation of the target pixel in LOS direction ($r'_{i\text{LOS}}$) are calculated. Using the measured movement and deformation of the target pixel in LOS direction ($r_{i\text{LOS}}$), the residuals of the target pixel are calculated ($v_i = r_{i\text{LOS}} - r'_{i\text{LOS}}$) and the error function of the parameter is constructed ($\varepsilon(B) = \sum |v_i|$). Then based on the criteria ($\varepsilon(B) = \min$), all the probability integral parameters are obtained accurately by the SA method. The accuracy and robustness of the proposed method are verified by simulation experiments. At last, the predicted parameters of mining subsidence in 9310 working face of Nantun Coal Mine are calculated by this method, and the characteristics of probability integral parameters are analyzed.

Introduction

Differential interferometry SAR (D-InSAR) technology has become a research hot spot in the field of mining deformation monitoring with the advantages of all-weather monitoring, high precision, surface measurement, and low cost. However, how to comprehensively calculate predicating parameters of probability integral based on D-InSAR technology is one of the core and difficult problems in data processing of D-InSAR mining deformation monitoring. Currently, the single-LOS D-InSAR technology is mainly

used to monitor mining subsidence, and unable to get the horizontal movement (Li et al. 2015). Therefore, the current D-InSAR monitoring results can only get the probability integral parameters related to subsidence (subsidence coefficient q, angle of maximum subsidence θ, tangent of major influence angle $\tan\beta$, and deviation of inflection point S), while the probability integral parameter (horizontal movement factor b) related to the horizontal movement cannot be obtained, which seriously restricts the popularization and application of D-InSAR technology in mine deformation monitoring.

There are two effective methods to solve the above problems. One is to establish three-dimensional InSAR deformation monitoring methods of InSAR which are suitable for mining subsidence characteristics, and then calculate the parameters comprehensively (hereafter referred to Method 1). The other way is to seek the model about the relationship among mining subsidence, horizontal movement, and deformation along LOS direction based on the single-LOS D-InSAR technology, and then to get the parameters by nonlinear theory (hereafter referred to

✉ Lei Wang
austwlei@163.com

✉ Nan Li
austlinan@163.com

1 School of Geodesy and Geomatics, Anhui University of Science and Technology, Huainan 232001, China

2 Key Laboratory for Land Environment and Disaster Monitoring of SBSM, China University of Mining and Technology, Xuzhou 221116, China

Method 2). The solutions of Method 1 include the integration of measurements from multi-sensor and/or multi-track D-InSAR (Fan et al. 2015a, b; Gray 2011; Wright et al. 2004; Hu et al. 2013a; Samsonov et al. 2013; Du et al. 2017), D-InSAR and offset tracking (Fialko et al. 2005; Hu et al. 2010; Fan et al. 2015a), D-InSAR and multi-aperture interferometry (Jung et al. 2011; Hu et al. 2014), D-InSAR and GPS (Gudmundsson et al. 2002; Samsonov and Tiampo 2006; Hu et al. 2013; Catalao et al. 2011; Gisinger et al. 2015), D-InSAR and SBAS/or PS (He et al. 2015; Bányai et al. 2016; Zhao et al. 2016), the earth's surface prior model and D-InSAR (Gourmelen et al. 2011; Guglielmino et al. 2011). However, all of these solutions focused on movement and deformation problems of earthquake, landslide, volcano eruption, and glacier movement, which are different from mining subsidence in movement mechanism. Therefore, these solutions can't solve the surface three-dimensional deformation monitoring caused by mine mining appropriately. In Li Zhiwei et al.'s pioneer work, combined with the conventional mining subsidence model, the three-dimensional deformation extraction method based on single-LOS D-InSAR technology has been put forward creatively by using the relationship between horizontal movement and subsidence gradient (Li et al. 2015). However, this approach is only applicable to mining subsidence monitoring in horizontal coal seam and gently inclined coal seam and is not available for special geological mining conditions such as inclined coal seam and steeply inclined coal seam, mountain areas, and so on. Therefore, further studies are needed for Method 1 to obtain the parameters of probability integral. For Method 2, studies show that although the methods based on single-LOS D-InSAR technology can't directly monitor the three-dimensional deformation of mining subsidence, the essence of the deformation in LOS direction is the sum of the projection of the subsidence component and horizontal movement component of target points along the LOS direction. Therefore, theoretically, according to this relationship model, combining with geological mining conditions of target area, the probability integral parameters can be inversed by nonlinear programming theory.

Based on the above analyses, the key researches of Method 2 are carried out in this paper. Based on laws of mining deformation and the geometrical imaging characteristics of radar, a new parameters inversion model of mining subsidence prediction is established by SA based on deformation in D-InSAR LOS direction. Then the simulation experiments are carried out to study its feasibility. Finally, the research achievements are applied for parameters inversion of probability integral in 9310 working face in Nantun Coal Mine of Yanzhou mining area. The research achievements are of great reference values for D-InSAR mine deformation monitoring.

The remainder of the paper is organized as follows. The methodology of subsidence prediction parameters inversion model using simulated annealing based on single line of sight D-InSAR is illustrated in Section 2. The simulated and real data experiments are carried out in sections three and four, followed by the discussion in section five. Section six presents the conclusions.

Methodology

Construction of parameter cost function of simulated annealing algorithm

When the satellite returns to the top of the target subsidence basin, assuming that the cumulative values of displacement and deformation at any pixel i in the mobile basin is $r_{i\mathrm{LOS}}$ (which can be obtained according to the deformations of each period in LOS direction), the subsidence value W_i, the horizontal movement to the north $U_{i\mathrm{SN}}$ and the horizontal movement to the east $U_{i\mathrm{EW}}$ can be predicted based on model of probability integral method and parameter system. According to the D-InSAR one-dimensional LOS projection principle (Hu 2012) (as shown in Fig. 1 where the arrow direction represents the positive direction), the predicting movement and deformation value $r'_{i\mathrm{LOS}}$ of any pixel i along the LOS direction can be expressed as formula (4):

According to the mining subsidence prediction model (taking the rectangular working face as an example), we can get the values of W_i, $U_{i\mathrm{SN}}$ and $U_{i\mathrm{EW}}$:

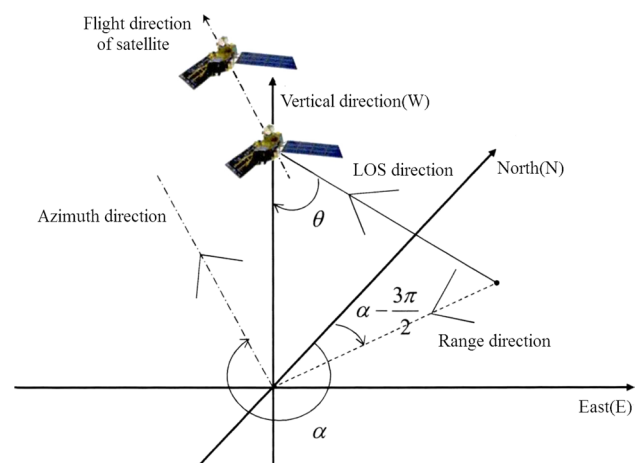$$W_i = W_{(x_i, y_i)} = \frac{1}{W_0} W^0_{(x_i)} W^0_{(y_i)} \tag{1}$$

Fig. 1 Principle diagram of D-InSAR one-dimensional LOS projection (Hu 2012)

$$U_{i\text{SN}} = U_{(x_i, y_i, \varphi_{i\text{SN}})} = \frac{1}{W_0}\left[U_{(x_i)}^0 W_{(y_i)}^0 \cos\varphi_{i\text{SN}} + U_{(y_i)}^0 W_{(x_i)}^0 \sin\varphi_{i\text{SN}}\right] \tag{2}$$

$$U_{i\text{EW}} = U_{(x_i, y_i, \varphi_{i\text{EW}})} = \frac{1}{W_0}\left[U_{(x_i)}^0 W_{(y_i)}^0 \cos\varphi_{i\text{EW}} + U_{(y_i)}^0 W_{(x_i)}^0 \sin\varphi_{i\text{EW}}\right] \tag{3}$$

In the formulas,

W_0: maximum surface subsidence value under full mining conditions; $\phi_{i\text{SN}}$ and $\phi_{i\text{EW}}$: respectively, from north to east, clockwise rotation to the prediction coordinate system x axis angle; $W_0(x_i)$: the subsidence value of the point with the abscissa of x_i on the main section when the sloping direction of working face is critical or supercritical; $W_0(y_i)$: the subsidence value of the point with the abscissa of y_i on the inclination main section when the tendency direction of working face is critical or supercritical; $U_0(x_i)$: the horizontal movement value of the point with the abscissa of x_i on the main section when the sloping direction of working face is critical or supercritical; $U_0(y_i)$: the horizontal movement value of the point with the abscissa of y_i on the inclination main section when the tendency direction of working face is critical or supercritical.

The value of $r'_{i\text{LOS}}$ can be obtained according to the relationship between formula (1), (2), (3) and $r'_{i\text{LOS}}$. The formula is as follows:

$$r'_{i\text{LOS}} = -U_{i\text{SN}}\sin\theta_i \cos\left(\alpha_i - \frac{3}{2}\pi\right) \\ - U_{i\text{EW}}\sin\theta_i \sin\left(\alpha_i - \frac{3}{2}\pi\right) + W_i\cos\theta_i \tag{4}$$

where θ_i is the incidence angle; α_i is the satellite azimuth along flight direction.

Define the pixel's predicting moving residual v_i along LOS direction as the following formula.

$$v_i = r'_{i\text{LOS}} - r_{i\text{LOS}} \tag{5}$$

where $r_{i\text{LOS}}$ and $r'_{i\text{LOS}}$ are the true deformation value and predicting deformation value of any pixel i in the moving basin along LOS direction, respectively.

Then the parameter cost function of simulated annealing algorithm can be expressed as:

$$F(X) = \sum_{i=1}^{n} v_i \tag{6}$$

The nature of obtaining parameters with SA is to seek a set of probability integral parameters X which can realize the minimum sum of absolute values of the difference between the predicting values and measured values of all the pixels' movement to LOS direction, that is $F(X) = \sum_{i=1}^{n} v_i = \min$.

Calculation model of probability integral parameters

SA is an algorithm for solving large-scale combinatorial optimization problems based on the principle of solid annealing. Based on the Metropolis acceptance criterion, SA uses probability search pattern in the solution space to seek optimal solution for objective function value. Based on the initial given solutions and parameters, the target solution is searched in solution space randomly, which makes the algorithm jump out of the local optimal solution and realize the global optimal solution (Wang et al. 2008). According to the principle of SA and the obtained cost function above, the full parameters inversion model of probability integral with SA and D-InSAR LOS direction is further established. The specific ideas of obtaining the parameters are as follows:

1. Preparatory work. The preparatory work includes to select the cost function $F(X)$, set the performing parameters of performing the SA (initial temperature $T = 400$, final temperature $T' = 5$, cooling coefficient $\alpha = 0.95$, neighborhood correlation factor S, and adaptive coefficient $b = 0.95$) and collect geological and mining conditions of working face, the deformation values of surface along D-InSAR LOS direction and choose the initial value X of probability integral parameter randomly to calculate the initial solution F_0 of the function.
2. To determine if $T < T'$, if yes, then output X. Otherwise, (3) to (6) will be executed.
3. If the number of internal recycle is met, then $T = T*\alpha$ and return (2); If not, then enter (4).
4. The generated adjacent scheme is $X' = (X_0', X_1' \dots X_7')^{\text{T}}$ and $X' = X + S*rnd$, where rnd is a random number between 0 and 1. The rule of S is $S' = b*S$, where b is a real number between 0 and 1.
5. According to the generation adjacent scheme, the objective function or fitness value F and the value of variable ΔF can be obtained. If $\Delta F \leq 0$ or $\exp(-\Delta F/T) \geq rnd$, then the new solution should be accepted, namely $X = X'$. Otherwise, the original solution should be kept and continue iteration, namely to reject the new solution and return (3).
6. To determine whether the external circulation criteria are satisfied (that is whether the minimum temperature is met), if yes, then output the probability integral parameters $X = (X_0, X_1 \dots X_7)$ which is the global optimal solution. Otherwise, the cooling equation $T_{k+1} = \alpha*T_k$ will be used (α is cooling coefficient from 0 to 1) and the (5) will be returned and executed.
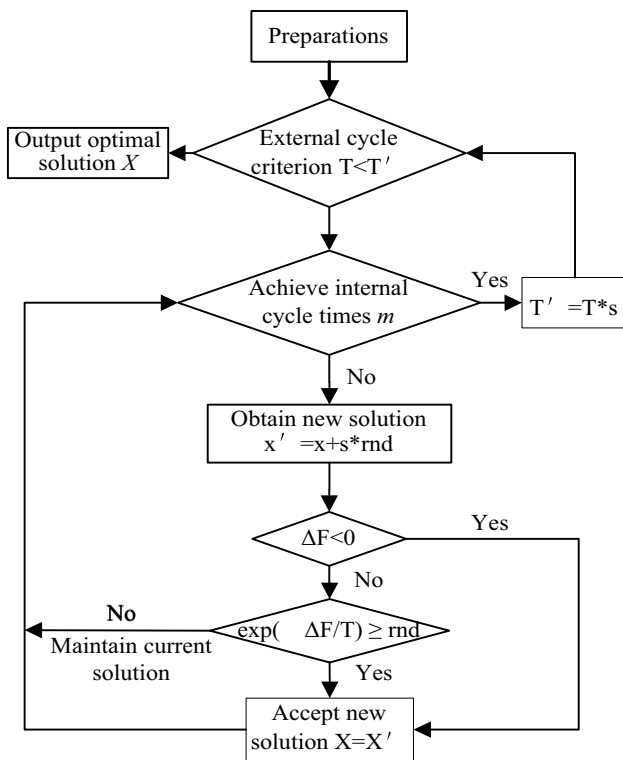
The flowchart of obtaining parameters is shown in Fig. 2.

Simulated experiment

Data simulation

Taking coal measures strata in Huainan mining area as background, the lithology of overlying strata in simulated working face is medium hard, the dip angle of coal seam is 8°, the mining height M is 3.0 m, and the mining depth H is 500 m. The projection mining dimension of the working face which is set along strike is $D_1 \times D_3 = 300\ m \times 500\ m$ along the dip and strike. The dip azimuth is 180°. The long-wall collapse method is used to control the roof. The mining degree of the working face meets $D_1/H = 0.6 < 1.2$–1.4 and

Fig. 2 Flowchart of probability integral parameter inversion model based on single-LOS D-InSAR and simulated annealing algorithm

$D_3/H = 1 < 1.2$–1.4, which caused mining of the working face along the dip and the strike are all to be non-full mining. Thus, the whole mining belongs to non-full mining. The true values of the probability integral parameters of the mining subsidence prediction in the simulated working face are shown in Table 1.

The incidence angle of radar θ is assumed to be 44.494°, and the azimuth of satellite LOS direction α is assumed to be 350.596° during the imaging of SAR satellite (Taking TerraSAR as an example). In order to simulate the accumulative D-InSAR deformation along the LOS direction caused by working face mining, the resolution of 10 m D-InSAR deformation map (azimuth and range direction to multi-view processing about 1:3) is obtained by dividing into north–south and east–west grids with an interval of 10 m on surface above the working face firstly. Then the grid point's subsidence W_i, the horizontal movement to the north U_{iSN}, and the horizontal movement to the east U_{iEW} can be predicted according to the established model by probability integral method and true values of parameters. The target points' cumulative movement along LOS direction can be calculated by formula (4), which can be used to simulate the measured cumulative movement amount in D-InSAR LOS direction. The simulation effect drawings are shown in Fig. 3.
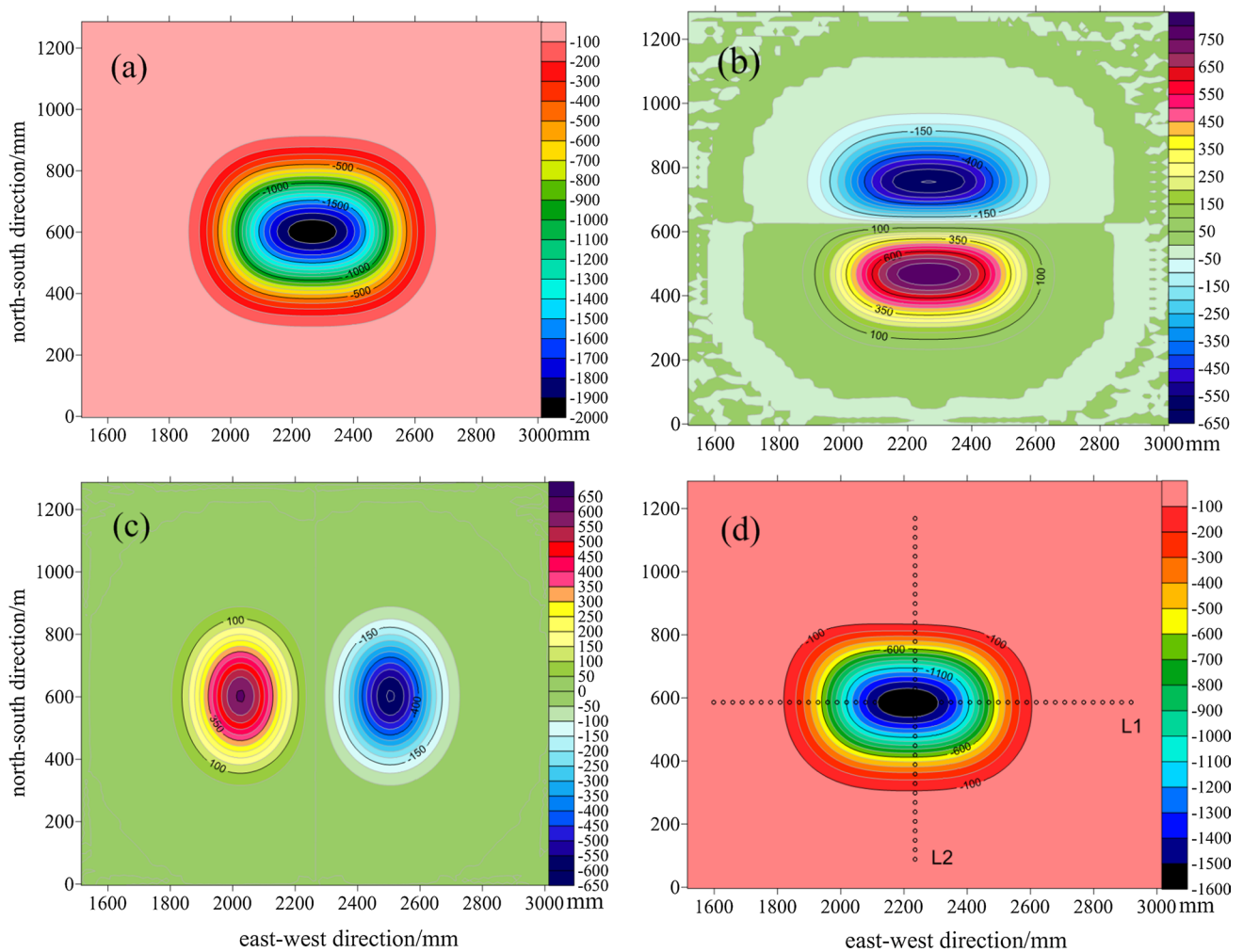
Analyses of experimental results

In order to verify the feasibility of parameters model, first select the arbitrary initial values in the vicinity of the true values of parameters (In engineering practice, the initial values of parameters are determined by the empirical relationship between the geological mining conditions and the probability integral parameters). Then the predicting parameters inversion is performed by the established probability integral parameter inversion model with D-InSAR LOS deformation and SA based on the simulation of movement and deformation values in D-InSAR LOS direction. If the new probability integral parameters are close to the true parameters values, the established probability integral parameter inversion model is effective and feasible.

Table 1 Parameters calculation results of simulation experiment

Name	Subsidence coefficient (q)	Tangent of major influence angle $(\tan \beta)$	Horizontal movement factor (b)	Angle of maximum subsidence $(\theta/°)$	Deviation of inflection point $(S_1/S_2/S_3/S_4/m)$
True values of parameters	0.800	2.00	0.30	85	10/10/10/10
Initial values of parameters	0.750	2.20	0.25	83	15/5/20/25
Inversion parameters	0.799	2.00	0.30	85	10/9/10/10
Errors analyses					
Absolute errors	0.001	0	0	0	0/− 1/0/0
Relative errors	1.25%	0%	0%	0%	0%/− 10%/0%/0%

Fig. 3 Data distribution of simulation experiments. **a** Simulated subsidence, **b** simulation of horizontal movement in north–south direction, **c** simulation of horizontal movement in east–west direction, **d** simulated movement in LOS direction

According to the layout of the surface movement observation station in conventional coal mining, the simulation observation line L_1 and L_2 are designed along the strike and dip of the working face, respectively. And 124 discrete points are selected with an interval of 30 m to calculate parameters of probability integral. Combining with the simulated movement and deformation values along the LOS direction by L_1 and L_2, as well as setting initial values of arbitrary parameters ($q = 0.750$, $\tan \beta = 2.20$, $b = 0.25$, $\theta = 83°$, $S_1 = 15$, $S_2 = 5$, $S_3 = 20$, $S_4 = 25$), the parameters are obtained by using the established parameter model. Table 1 shows the parameters of calculation, while Fig. 4 shows the fitting results.

The results in Table 1 show that the parameter values ($\tan \beta$, b, θ, S_1, S_3, and S_4) are entirely consistent with true values. The relative error of q is 1.25%, while the relative error of S_2 is slightly larger but no more than -10% (which has small impact on the whole effect). As seen in Fig. 4, the fitting

errors are between -3 and 2 mm, while the mean square error is ± 0.64 mm. Therefore, without considering the deformation errors in LOS direction, the established model can accurately reverse the predicting parameters of probability integral, which verifies the feasibility of the model.

Real data experiment

Introduction of experiment area and radar data

The experiment area is located in No. 9 mining area of Nantun Coal Mine in Yanzhou coalfield. The Zouji Highway and mining railways pass over the experiment area. During the Dec. 25, 2011 to Mar. 11, 2012 (radar data coverage period), the west section of 9310 working face and the east section of 9308 working face in 3 upper coal seam are mining. The old goafs have formed and the

Fig. 4 Diagram of parameters fitting effect
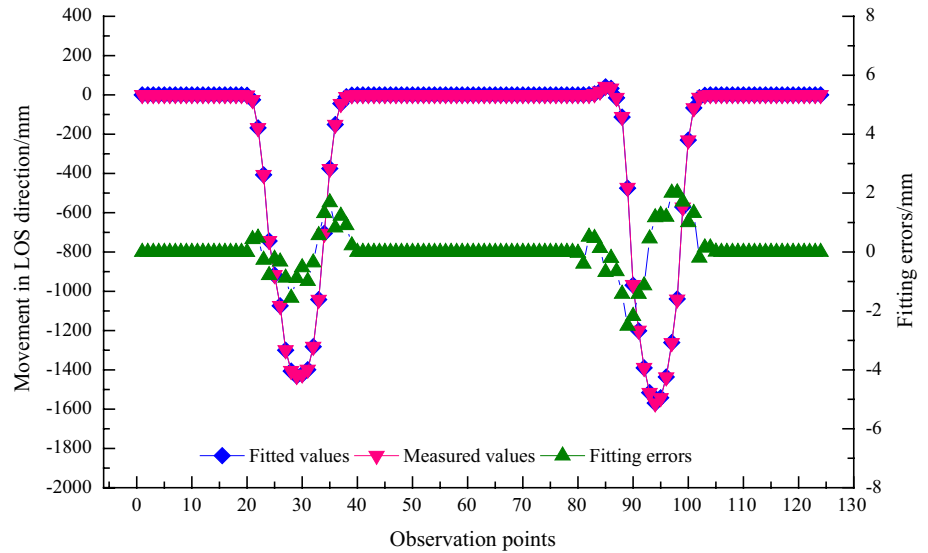
surface subsidence was basically stable when the mining of the north section of 9310 working face and the south section of 9308 working face was finished. The coal seams in 9310 and 9308 working face are flat coal seams with average of angle 8°. The working face is arranged along the strike, and the fully mechanized caving coal mining is used for excavation. The coal seam thickness of the 9310 working face is 4.90 m, the mining depth is 588 m, and the length of the working face is 197 m. During the experiment period, the advanced length of 9310 work face is approximately 220 m. The coal seam thickness of the 9308 working face is 4.76 m, the mining depth is about 630 m, and the length of working face is 140 m. During the experiment period, the advanced length of 9310 work

face is approximately 415 m. The geographical location and optical image of this test area are shown in Fig. 5. It shows that the 9308 and 9310 working face and some goafs as well as the advance of the working faces in Fig. 6 (Show only the old goaf 9312 and 9306 adjacent to the easilymined "activated" goaf).

The experimental data are single look complex (SLC) radar images obtained by TerraSAR-X with the resolution of 3 m and the image size of 16,224 × 10,710 pixels. The experimental data cover the whole Nantun Coal Mine. Considering that the large deformation gradient of the mining area can cause the spatial decorrelation, seven scene SAR images with time baselines of 11 days and 22 days from Dec. 25, 2011 to Mar. 11, 2012 were selected for the experiment.
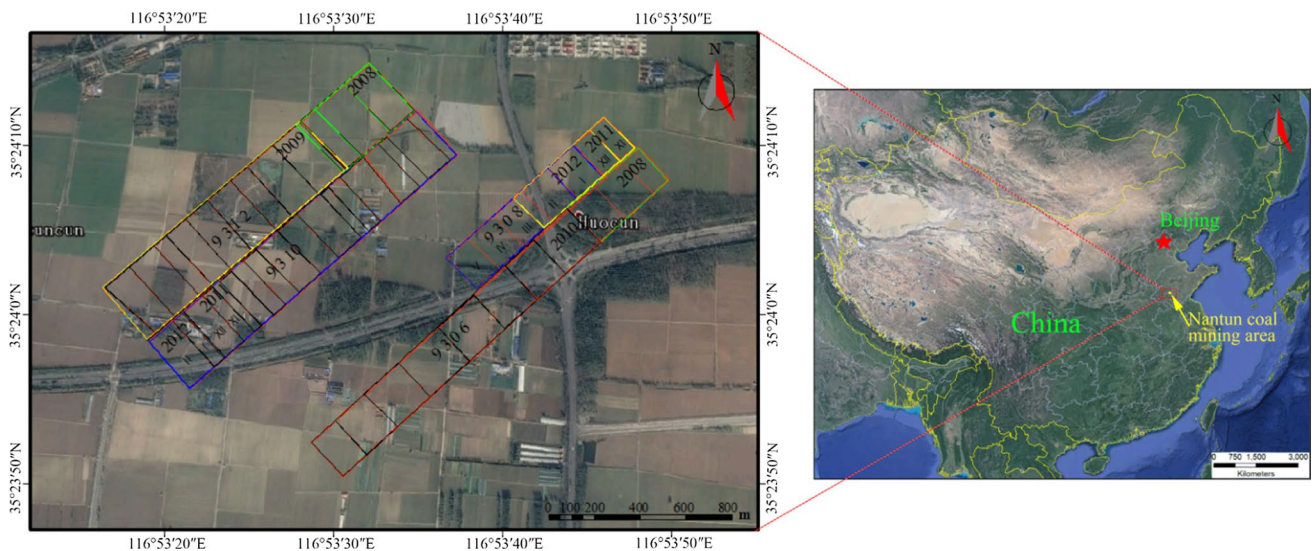
Fig. 5 Location of the Nantun coal mine

Table 2 shows the main geometrical parameters and differential interference schemes of TerraSAR-X images.

Research on inversion of probability integral parameters

The amount of surface movement and deformation of each interference pair along the LOS direction has been obtained by using differential interferometry for 6 pairs of master–slave images in Table 3, respectively. Because each interference pair has same azimuth in LOS direction and the incident angles are approximately equal (which can be considered the same, so that the error can be neglected), the accumulative surface movement and deformation maps along LOS direction in six time periods of the relative and reference time (Dec. 25, 2011) has been obtained by adding up the movement and deformation of each interference pair along LOS direction, as shown in Fig. 6.

Taking 9310 working face as an example, it has stopped excavation in Feb. 28, 2012. By the end of Mar. 11, 2012, although the surface moving basin hasn't become stable, it is possible for approximate inversion of dynamic probability integral parameters of moving basin on Mar. 11. As a result

of the 9310 working face is rectangular in shape and the coal seam is nearly horizontal, the mining subsidence basin is symmetrical. Therefore, we can select half line C along the west of the strike direction and half line D along the south of the dip direction respectively, as shown in Fig. 7f. And assume that the working face mining before Dec. 25, 2011 has no superimposed influence on the deformation of line C and line D. The probability integral parameters inversion can be conducted with the combination of any arbitrary initial values (The initial values in the paper are $q = 0.200$, tan $\beta = 2.00$, $b = 0.20$, $\theta = 88°$, and $S_1 = S_2 = S_3 = S_4 = 0$) and the movement and deformation along LOS direction of line C and line D.

The results show that the dynamic prediction probability integral parameters of mining subsidence at 9310 working face on Mar. 11 are as follows: $q = 0.188$, $b = 0.11$, $\tan\beta = 2.0$, $\theta = 88°$, $S_1 = -10$, $S_2 = 10$, $S_3 = -80$, $S_4 = 33$ and the fitting mean square error is ± 18.31 mm. The fitting effect is shown in Fig. 7.

The results show that the deviation of upper inflection point offset in 9310 working face has reached -80 m ($S_3 = -80$ m). This is mainly due to the existence of large cantilever beam or masonry beam in the downhill direction

Table 2 Geometric parameters of TerrraSAR-X images and differential interference schemes

Interference pairs	Master images	Slave images	Time baseline/d	Vertical baseline/m	Incident angles of master image/°	Azimuth/°
1	20,111,225	20,120,105	11	−25.10	44.4974	350.596
2	20,120,105	20,120,116	11	105.60	44.5000	350.596
3	20,120,116	20,120,127	11	6.43	44.4893	350.596
4	20,120,127	20,120,207	11	90.50	44.4940	350.596
5	20,120,207	20,120,218	11	−141.72	44.4831	350.596
6	20,120,218	20,120,311	22	−19.63	44.4961	350.596

Table 3 Inversion results of parameters after adding random errors

| Name	Subsidence coefficient (q)	Tangent of major influence angle ($\tan\beta$)	Horizontal movement factor (b)	Angle of maximum subsidence ($\theta/°$)	Deviation of inflection point ($S_1/S_2/S_3/S_4$/m)	Fitting errors/mm
True values	0.800	2.00	0.30	85	10/10/10/10	–
Plus 0 mm	0.799	2.00	0.30	85	10/9/10/10	0.64
Plus 5 mm	0.793	2.01	0.30	85	10/10/10/10	4.48
Plus 10 mm	0.792	2.01	0.30	85	10/10/11/11	8.83
Plus 15 mm	0.786	2.02	0.30	85	10/10/13/10	13.23
Plus 20 mm	0.781	2.04	0.30	85	10/10/15/10	17.65
Plus 25 mm	0.776	2.05	0.30	85	10/10/15/11	22.05
Plus 30 mm	0.775	2.04	0.30	85	10/10/16/11	26.49
Plus 35 mm	0.769	2.06	0.30	85	10/10/16/12	30.91
Plus 40 mm	0.763	2.07	0.30	84	10/10/18/10	35.36
Plus 45 mm	0.764	2.06	0.30	84	10/10/19/11	39.82
Plus 50 mm	0.757	2.09	0.30	85	10/10/18/14	44.19
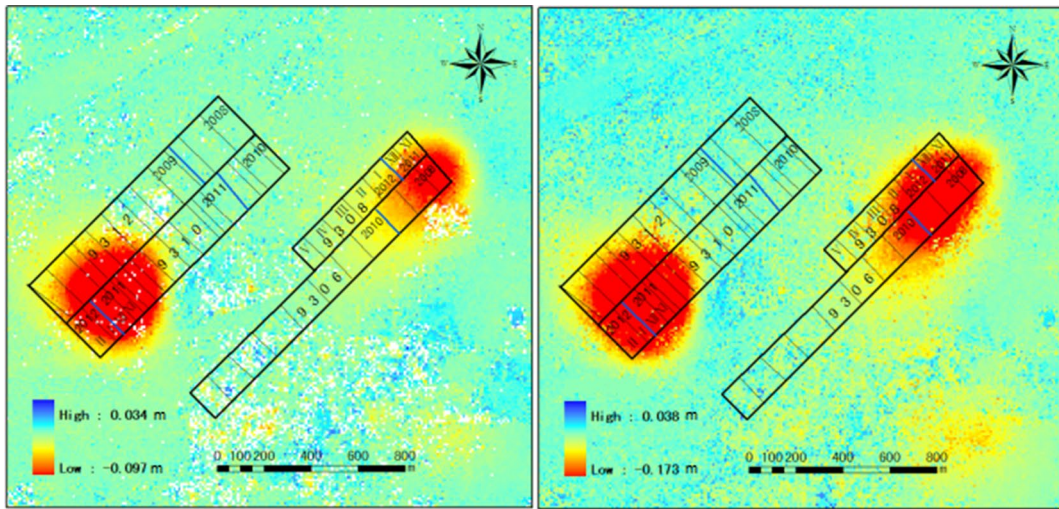
(a) Dec. 25, 2011-Jan. 5, 2012

(b) Dec.25, 2011-Jan.16, 2012
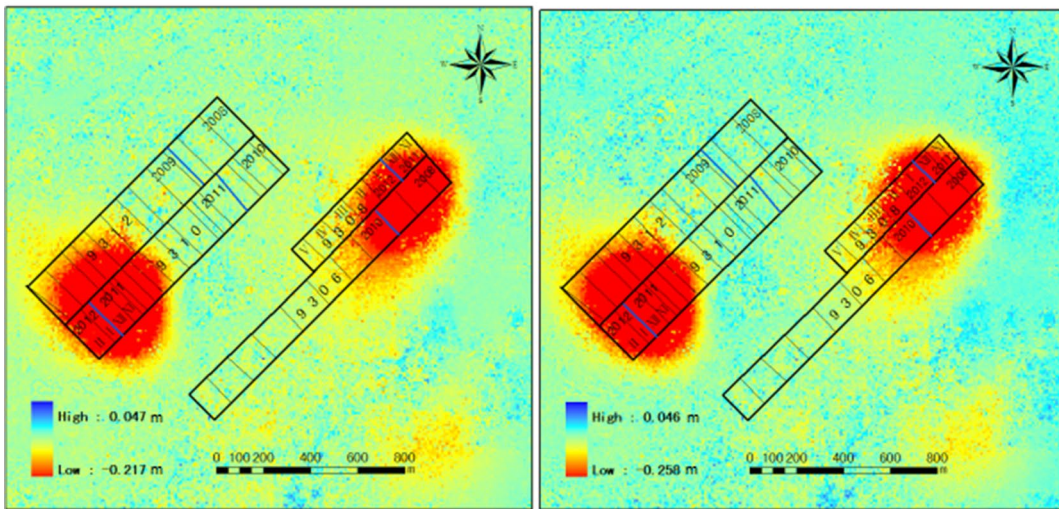
(c) Dec.25, 2011-Jan.27, 2012

(d) Dec.25, 2011-Feb.7, 2012
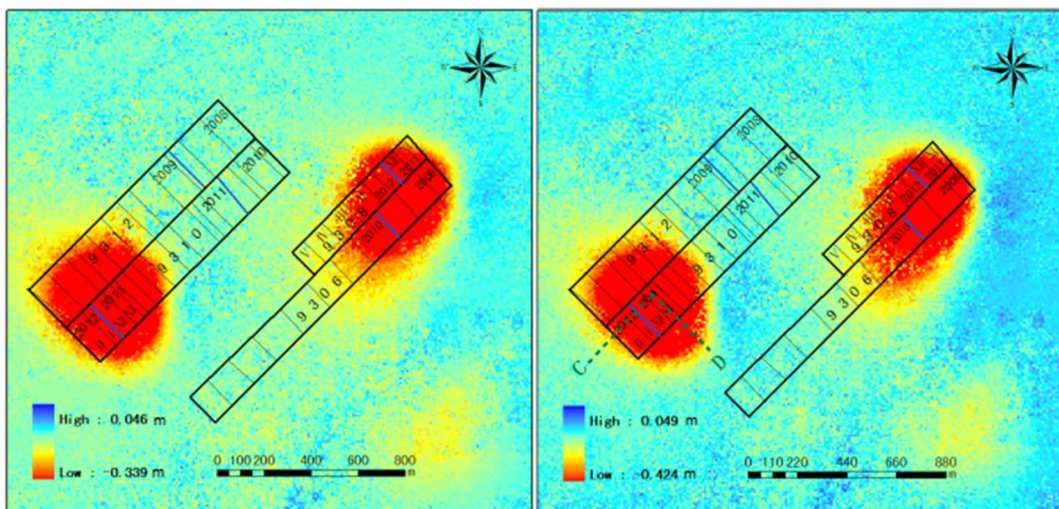
(e) Dec.25, 2011-Feb.18, 2012

(f) Dec.25, 2011-Mar.11, 2012

◀**Fig. 6** Accumulative surface movement and deformation in LOS direction at each period. **a** Dec. 25, 2011–Jan. 5, 2012, **b** Dec. 25, 2011–Jan. 16, 2012, **c** Dec. 25, 2011–Jan. 27, 2012, **d** Dec. 25, 2011–Feb. 7, 2012, **e** Dec. 25, 2011–Feb. 18, 2012, **f** Dec. 25, 2011–Mar. 11, 2012

of 9312 working face which loses its stability during the mining of 9310 working face. Other probability integral parameters are basically normal.

Discussion

The measurement error of D-InSAR is inevitable due to the limitation of the measurement environment conditions. In order to study the robustness of the algorithm in this paper, under the simulated experimental conditions in Chapter 3, the random error of 0–50 mm (as shown in Table 3) is added to the deformation along D-InSAR LOS direction in order of 5 mm interval. The robustness of the proposed algorithm is evaluated by solving the relative error and the deformation fitting error along LOS direction of the parameters which are obtained by the proposed algorithm. The results of calculating the parameters and robustness of each scheme are shown in Table 3.

It can be seen from Table 3 that: (1) The error of q and tan β increases gradually with the increase of deformation error along D-InSAR LOS direction. When the error of the observation value is 50 mm, the relative error of q is only 5.4% and the relative error of tan β is only 4.5%. (2) When the observation errors are in the range of 5 mm to 50 mm, the values of b and θ fit well with the true values, which indicate that the deformation error along D-InSAR LOS direction basically has no influence on model performance. (3) When the observation errors are in the range of 5 m–50 mm, the results of S_1, S_2, and S_4 are basically in consistent with true values. With the increase of observation error, the parameter error of S_3 increases gradually, but has small effect on the whole results (the fitting error is small). The robustness experiment shows that the established full probability integral parameters inversion model with single-LOS D-InSAR and SA in this paper has good performance. The model robustness performance is shown in Fig. 8.

Conclusions

Due to the inability of the single line of sight D-InSAR to monitor the three-dimensional deformation of the surface, the conventional methods are unable to obtain the

prediction parameters (probability integral parameters) of surface subsidence in coal mining. In this paper, the researches on solving all the probability integral parameters by using simulated annealing based on single line of sight D-InSAR are carried out. And the main achievements are as follows.

1. A calculation method of simulated annealing for probability integral parameters based on single line of sight D-InSAR is proposed. Firstly, the method predicts the subsidence, the horizontal movement in the north–south direction and the horizontal movement in the east–west direction of the target pixel by using the probability integral method. Based on the projection relationship between the three-dimensional deformation and the LOS deformation, the predicted movement and deformation of the target pixel in LOS direction (r'_{iLOS}) are calculated. Using the measured movement and deformation of the target pixel in LOS direction (r_{iLOS}), the residuals of the target pixel are calculated ($v_i = r_{iLOS} - r'_{iLOS}$) and the error function of the parameter is constructed ($\varepsilon(B) = \sum |v_i|$). Then based on the criteria ($\varepsilon(B) = \min$), all the probability integral parameters are obtained accurately by the simulated annealing method. And the procedure for calculating parameters is also compiled.

2. The simulation experiments results show that, the relative errors of q, tanβ, b and θ calculated by this method are not more than 1.25%, and the relative error of deviation of inflection point S is not more than -10%; the fitting errors of calculate parameters are between -5.9 mm and 6.1 mm, while the mean square error is about ± 0.64 mm. When the adding measurement error reaches 50 mm, the relative errors of q and tanβ are, respectively, 5.4 and 4.5%, and the relative errors of b and θ are all zero, and the effect of partial deviation of inflection point S is slightly poor (but less effect on the fitting result). The method in this paper has good performance on robustness.

3. The application experiment shows: the dynamic probability integral parameters of mining subsidence in 9310 working face on Mar. 11, 2012 are calculated, and the results are as follows: $q = 0.188$, $b = 0.11$, tan$\beta = 2.06$, $\theta = 88°$, $S_1 = -10$, $S_2 = 10$, $S_3 = -80$, $S_4 = 33$, while the deformation fitting mean square error along LOS direction is ± 18.31 mm. It is considered that $S_3 = -80$ is mainly owing to the instability of cantilever beam or masonry beam in the boundary of the adjacent 9312 goaf caused by mining of 9310 working face.
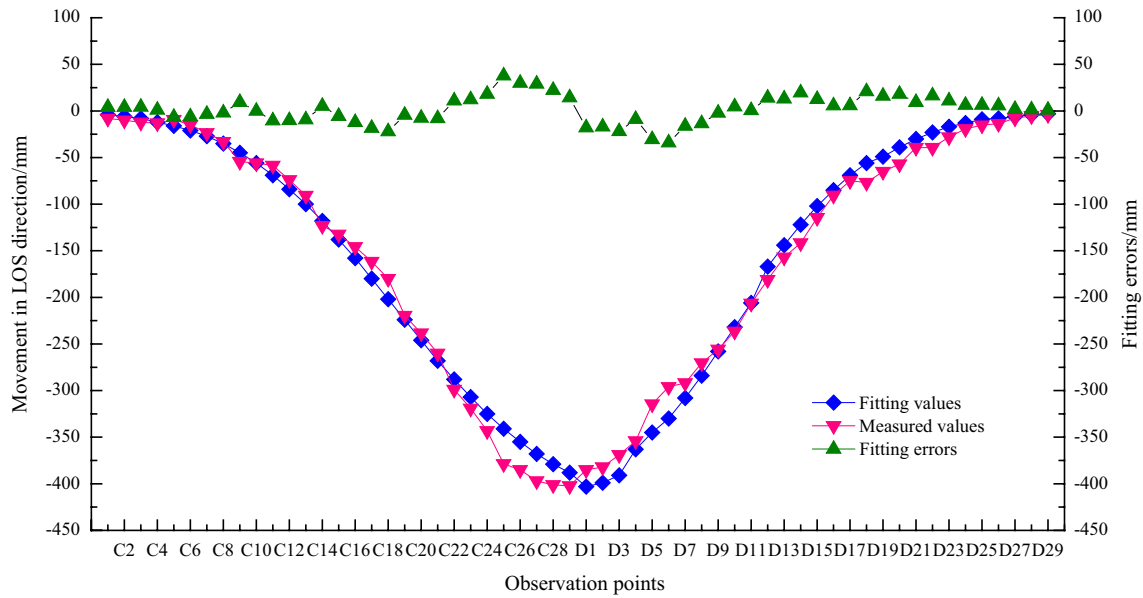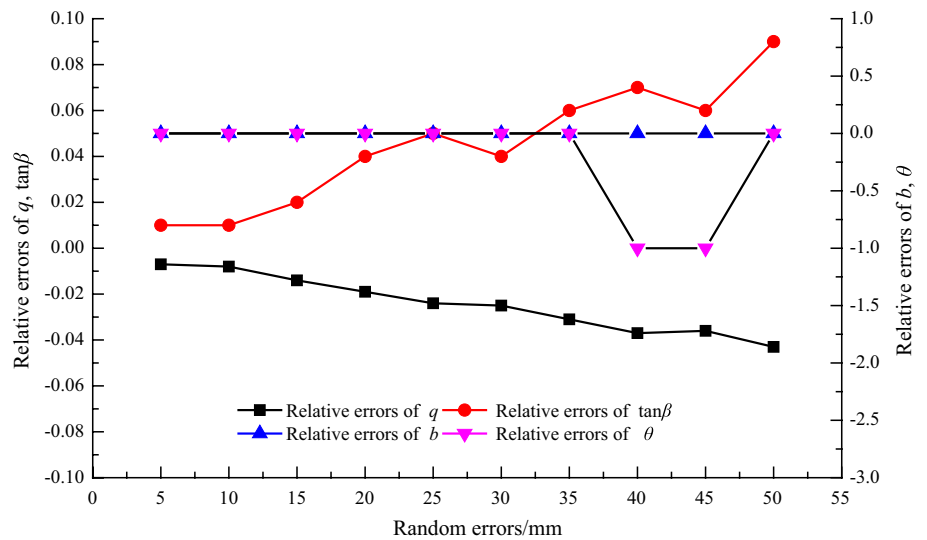
Fig. 7 Diagram of parameters fitting effect

Fig. 8 Relative errors of each inversion parameters with random errors

References

Bányai L, Szűcs E, Wesztergom V (2016) Geometric features of LOS data derived by SAR PSI technologies and the three-dimensional data fusion. Acta Geod Geoph 52(3):421–436

Catalao J, Nico G, Hanssen R et al (2011) Merging GPS and atmospherically corrected InSAR data to map 3-D terrain displacement velocity. IEEE Trans Geosci Remote Sens 49(6):2354–2360

Du Y, Zhang L, Feng G et al (2017) On the accuracy of topographic residuals retrieved by MTInSAR. IEEE Trans Geosci Remote Sens 99:1–13

Fan H, Gao X, Yang J et al (2015a) Monitoring mining subsidence using a combination of phase-stacking and offset-tracking methods. Remote Sens 7(7):9166–9183

Fan HD, Cheng D, Deng KZ et al (2015b) Subsidence monitoring using D-InSAR and probability integral prediction modelling in deep mining areas. Surv Rev 47(345):438–445

Fialko Y, Sandwell D, Simons M et al (2005) Three-dimensional deformation caused by the Bam, Iran, earthquake and the origin of shallow slip deficit. Nature 435:295–299

Gisinger C, Balss U, Pail R et al (2015) Precise three-dimensional stereo localization of corner reflectors and persistent scatterers with TerraSAR-X. IEEE Trans Geosci Remote Sens 53(4):1782–1802

Gourmelen N, Kim SW, Shepherd A et al (2011) Ice velocity determined using conventional and multiple-aperture InSAR. Earth Planet Sci Lett 307(1):156–160

Gray L (2011) Using multiple RADARSAT InSAR pairs to estimate a full three-dimensional solution for glacial ice movement. Geophys Res Lett 38(38):132–140

Gudmundsson S, Sigmundsson F, Carstensen JM (2002) Three-dimensional surface motion maps estimated from combined interferometric synthetic aperture radar and GPS data. J Geophys Res Solid Earth 107(B10):ETG 13-1–ETG 13-14

Guglielmino F, Bonforte A, Puglisi G et al (2011) Analysis of satellite and in situ ground deformation data integrated by the SISTEM approach: the April 3, 2010 earthquake along the Pernicana fault (Mt. Etna-Italy) case study. EGU Gen Assem 2011:327–336

He L, Wu L, Liu S et al (2015) Mapping two-dimensional deformation field time-series of large slope by coupling DInSAR-SBAS with MAI-SBAS. Remote Sens 7(9):12440–12458

Hu J (2012) Theory and method of three-dimensional deformation estimation based on modern surveying adjustment. School of Earth Science and Information Physics, Central South University, Changsha

Hu J, Li ZW, Zhu JJ et al (2010) Inferring three-dimensional surface displacement field by combining SAR interferometric phase and amplitude information of ascending and descending orbits. Sci China (Earth Sci) 53(4):550–560

Hu J, Ding XL, Li ZW et al (2013) Kalman-filter-based approach for multisensor, multitrack, and multitemporal InSAR. IEEE Trans Geosci Remote Sens 51(7):4226–4239

Hu J, Li ZW, Li J et al (2014) 3-D movement mapping of the alpine glacier in Qinghai-Tibetan Plateau by integrating D-InSAR, MAI and offset-tracking: case study of the Dongkemadi Glacier. Global Planet Change 118(4):62–68

Jung HS, Lu Z, Won JS et al (2011) Mapping three-dimensional surface deformation by combining multiple-aperture interferometry and conventional interferometry: application to the June 2007 Eruption of Kilauea Volcano, Hawaii. IEEE Geosci Remote Sens Lett 8(1):34–38

Li ZW, Yang ZF, Zhu JJ et al (2015) Retrieving three-dimensional displacement fields of mining areas from a single InSAR pair. J Geodesy 89(1):17–32

Samsonov S, Tiampo K (2006) Analytical optimization of a DInSAR and GPS dataset for derivation of three-dimensional surface motion. IEEE Geosci Remote Sens Lett 3(1):107–111

Samsonov S, D'Oreye N, Smets B (2013) Ground deformation associated with post-mining activity at the French–German border revealed by novel InSAR time series method. Int J Appl Earth Obs Geoinf 23(8):142–154

Wang K, Gao X, Chen T (2008) Influencing factors for formation of urban and rural spatial structure in metropolis fringe area taking Shuangliu County of Chengdu in China as a Case. Chin Geogra Sci 18(3):224–234

Wright TJ, Parsons BE, Lu Z (2004) Toward mapping surface deformation in three dimensions using InSAR. Geophys Res Lett 31(1):169–178

Zhao R, Li ZW, Feng GC et al (2016) Monitoring surface deformation over permafrost with an improved SBAS-InSAR algorithm: with emphasis on climatic factors modeling. Remote Sens Environ 184:276–287